Optimal Control of Building HVAC Loads for Demand Response Participation

Aysegul Kahraman* and Emrah Biyik
Department of Energy Systems Engineering
Yasar University, Izmir, Turkey
e–mail: aysegul.kahraman@yasar.edu.tr, emrah.biyik@yasar.edu.tr

ABSTRACT

Buildings are responsible for about 40% of the global energy consumption, where heating, ventilation and air conditioning (HVAC) systems account for the most part of it. Continuous increase in use of the HVAC systems and required power may cause overload in the electric power grid, and may result in power outages, as well as increased utility bills to the building dwellers. Therefore, in order to help the grid operations, and to mitigate such adverse situations, efficient use of HVAC equipment is of utmost importance.

In this paper, an optimal control framework utilizing HVAC system efficiently to reduce both energy consumption and peak load demand is developed. To achieve this, a mathematical model that describes the zone transient thermal dynamics is obtained using real measurement data. Next, a model predictive control algorithm that takes into account building dynamic models and actual operational data to regulate building thermal comfort are developed in MATLAB. The generated algorithm looks ahead for a 24-hour period with a time step of 10-minute intervals. Thus, the controller considers the changes in the outside dry-bulb air temperature, electricity price, required energy amount and comfort conditions simultaneously in order to find the proper optimal zone temperatures guaranteeing user comfort in terms of the First-Law of Thermodynamics. The new controller was tested using data from a real building, and preliminary results indicate that significant reduction in peak electrical power demand can be achieved by the proposed approach depending upon operating conditions.

KEYWORDS

Peak load reduction, HVAC, demand response, model predictive control, thermal model, system identification

1. INTRODUCTION

The renewable energy penetration targets set by EU and US [1]-[2] necessitate a radical change in the way the electric power grid is operated. Conventional power grids were designed around dispatchable central power plants at a transmission level providing services down to industrial, commercial and residential end-users at a distribution level. Increased penetration of the intermittent and uncertain renewable energy sources effectively implies additional loads, which require generation flexibility at multiple time-scales to ensure safe and stable operation of the electric power grid. Since conventional generation is increasingly displaced by renewables, this additional flexibility can no longer be sourced solely from conventional plants. It needs to be managed also from the demand side (demand-side management).

According to the International Energy Agency [3], buildings are responsible for about 40% of the global energy consumption, and about 50% of the energy used in a typical building is accounted for the space heating, ventilation, and air conditioning (HVAC) system. The European Directive on the energy performance of buildings (EPBD) encourages the European

Union member states to approve energy policies that promote the implementation of very low and even close to zero energy buildings [4].

Improving operational efficiency of HVAC systems will result in large savings in the energy consumption. In addition, high thermal capacity of large commercial buildings allows real-time control of their HVAC systems to regulate electricity demand as required for grid stability, without effecting the quality of service in the building significantly. Therefore, buildings represent an opportunity as flexible loads that can be controlled to provide ancillary services to the electric power grid, and thus enable high penetration of renewables.

Traditionally, ancillary services in the power grid have been provided by fast ramping generation assets, which are costly to operate, and depend on fossil fuels. Recent advancements in communication and control capabilities of the power grid enabled demand side to provide high-quality ancillary services at various time scales [5]. Several approaches [6]-[8] for managing flexible loads depend on priority-based scheduling of loads modelled as a stochastic battery. Both Europe [9] and the US [10] are putting significant effort for large scale adaptation of building flexible loads as reliable contributors in the ancillary services market.

There are many flexible load types that can be tapped into for ancillary services, such as building HVAC, building and municipal lighting; electric vehicles; data centres (cooling); agricultural, residential (pool) and waste-water pumping; refrigerated warehouses, etc. In this paper, however, only the building HVAC loads are considered. This is a reasonable choice because HVAC corresponds to a very large share of the load in today's grid.

Building energy controls is a very active research area [11]. Simple on-off or logic-based control designs [5] fall short of extracting the full benefits provided by more sophisticated controls. Recently, several EU and US researchers reported advanced models of predictive control (MPC) techniques for building heating and cooling management [12]-[16]. In [12], authors propose a centralized stochastic control approach, where the controller accounts for the uncertainties in the ambient temperature. In another study [13], a distributed control architecture that computes optimal supply air temperature and flow rate is proposed. These advanced approaches, however, do not scale well as the number of zones in the building increases, and/or require a large investment in new control hardware for implementation. This poses a significant barrier for adoption of these methods by small and medium commercial buildings, because they usually lack the sophisticated control equipment, and more importantly financial incentive for upgrades due to long and uncertain return on investment. Therefore, a wider adoption of advanced building thermal control techniques can be achieved by developing solutions that are implementable on simple or already existing equipment. Another improvement opportunity as compared to [12] and [13], is the fact that they consider only controlling building zone temperatures within pre-determined bounds, without explicit consideration of the occupant comfort.

This paper introduces a new model of predictive controller (MPC) that (i) minimizes peak heating/cooling load on the HVAC equipment (ii) while achieving a satisfactory thermal comfort inside the building, and (iii) is capable of handling large-scale systems with uncertain dynamics (e.g. ambient air-temperature, internal heat gains, etc.). The key difference of our approach compared to previous approaches that utilize MPC is that in our approach the HVAC units are not controlled directly. Instead, the system is controlled indirectly by sending control inputs to the zone thermostats and thus requires minimal hardware changes. This renders our approach suitable for implementation in low-cost embedded platforms used in most of the HVAC control equipment.

The rest of the paper is organized as follows. In Section 2 the thermal model development process is described, followed by the controller formulation in Section 3. Application of the proposed study to a real building is presented in Section 4. Concluding remarks and future work are presented in Section 5.

2. MODEL DEVELOPMENT

In this section, the details of the mathematical model of the zone thermal dynamics and human comfort model as they apply to our controller design are described.

2.1 Zone Thermal Model

The thermal dynamics of an individual zone is modeled by a lumped resistance-capacitance circuit as shown in **Hata! Başvuru kaynağı bulunamadı.**. The model parameters are physics-based, and exact calculation of these parameters requires comprehensive details of the zones (construction material, insulation, etc.). To circumvent this, parameters are estimated from sensor measurements using system identification methods. These thermal models are then employed to predict the zone temperatures, power consumption, and thermal comfort in the building in response to thermostat set-point changes. Unlike previous studies where human comfort is mapped to a fixed temperature constraint, our optimization algorithm considers the human comfort model and, in effect, opens up the operating space of the HVAC system for more efficient operation.

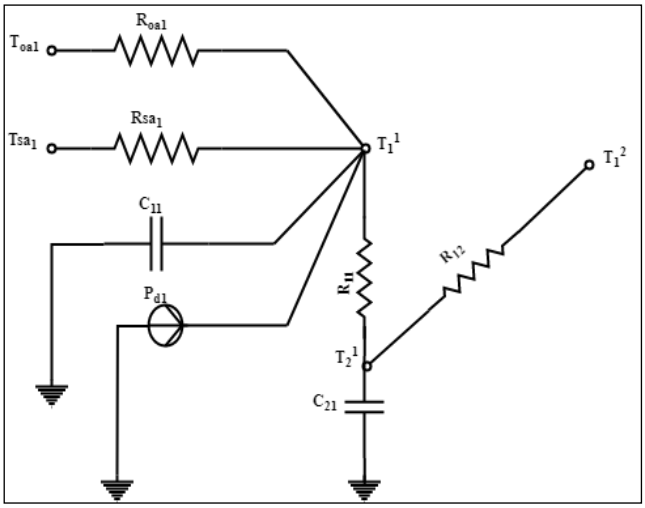

Figure 1. Lumped resistance-capacitance model of a thermal zone

Each zone is modelled as a two-mass system where the room air temperature acts as a fast-dynamic mass and solid parts (walls, furniture, etc.) as the slow-dynamic mass. The continuous time, linear, thermal dynamic model of a zone can be stated by the following set of differential equations:

$$C_1^j \dot{T}_1^j = \dot{m}^j C_p^j \left(T_{sa}^j - T_1^j\right) + \frac{T_2^j - \mathrm{T}_1^j}{R_1^j} + \frac{T_{oa} - \mathrm{T}_1^j}{R_{oa}^j} + \mathrm{P}_d^j \quad (1)$$

$$C_2^j \dot{T}_2^j = \frac{T_1^j - \mathrm{T}_2^j}{R_1^j} + \sum_{i \in N_j} \frac{T_1^i - \mathrm{T}_2^j}{R_{ij}} \quad (2)$$

where, T_1^j and T_2^j zone air and wall temperatures, C_1^j and C_2^j thermal capacitance, $\dot{m}^j$ supply air mass flow rate and C_p^j specific heat, T_{sa}^j supply air temperature, R_1^j thermal resistance between zone air and wall, R_{ij} thermal resistance between adjacent zones, N_j the set of zones adjacent to zone j, P_d^j the total internal disturbance heat gain (lighting, occupancy, solar gains, etc.), and T_{oa} the outside air temperature. It must be noted that Eq. (1) is related to the zone air temperature acting as a fast-dynamic mass, whereas Eq. (2) is related with the zone wall temperature as slow dynamic mass.

Buildings are typically comprised of multiple thermal zones as in Figure 2. In this case, for each zone j a suitable zone thermal model is developed, where the interaction between zones i and j are captured by the resistance term R_{ij}. Then, collection of these models ($j = 1, \dots, n_z$) are used to describe the overall thermal dynamics of the building.

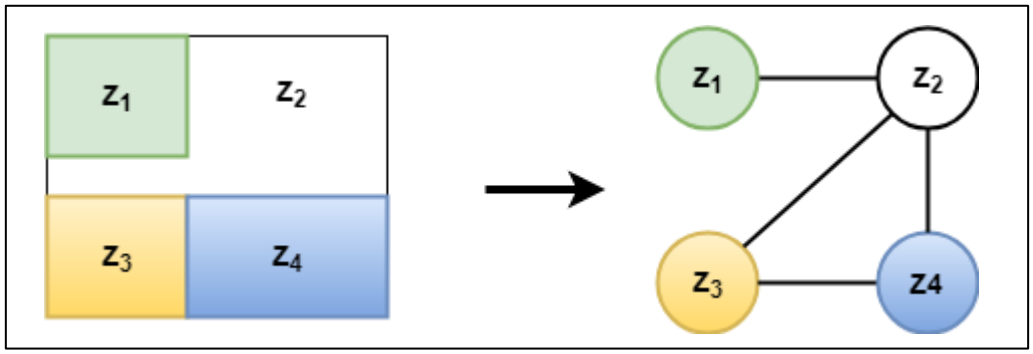

Figure 2. Multiple zone thermal model and its adjacency graph

The lumped parameters R and C are dependent on the building zone physics (construction material, window-to-wall ratio, equipment type, orientation, etc.) and calculation of their exact values requires significant amount of effort, and sometimes may be impossible for older retrofit buildings due to missing information. Thus, to enable a wider implementation of our approach, the values of R and C are identified using data collected from the zone. To achieve this, an unconstrained multivariable nonlinear optimization problem is solved such that the error between the measured zone air temperature and its estimated value from the model is minimized. For this purpose, the following optimization problem is formulated:

$$\min_{P=\{R,C\}} \frac{1}{N}\sum_{k=1}^{N}\sum_{j=1}^{n_z}\left(T_1^{j,m} - T_1^{j,e}(P,U)\right) \tag{3}$$

subject to Eqs. (1) and (2),

where P denotes the unknown parameter vector, k time step, N number of samples, n_z number of thermal zones, $T_1^{j,m}$ measured zone air temperature and $T_1^{j,e}(P,U)$ estimated zone air temperature from model, and U the heating/cooling input vector (due to supply air, ambient temperature and internal gains). It must be noted that the wall temperature is not included in the objective function, because most of the buildings would not be equipped with wall temperature sensors, and thus the data would not be available in retrofit applications.

2.2 Human Comfort Model

The fundamental goal of any HVAC control system is to achieve human comfort. In this paper, one of the earliest and widely accepted human comfort models attributed to Fanger [17] is used. Here, a brief description of the human comfort model as used in our controller design is provided. For a detailed discussion, the reader is referred to [18] and references therein. In Fanger's model, *predicted mean vote* is an empirical thermal sensation scale taking integer values ranging from -3 (cold) to 0 (neutral) to 3 (hot). The average value of predicted mean vote depends on the difference between metabolic rate M, external work W (0-0.2 M, [18]), and total heat loss L from Fanger's model [17], according to the empirical formula:

$$\alpha = (0.303\, e^{-0.036M} + 0.02)\,(M - W - L) \tag{4}$$

Predicted percent of dissatisfied occupants, denoted by γ, is related to α through another empirical relation:

$$\gamma = 100 - 95e^{-0.03353\alpha^4 - 0.2179\alpha^2}, \tag{5}$$

where the minimum value of γ is 5%, attained at $\alpha = 0$ (neutral). In our MPC formulation, γ is used as one of the objective terms, in addition to heating/cooling load, to be minimized. In other words, we use the combined model described by Eqs. (1), (2) and (4) to predict the thermal behavior of the zones and occupant comfort. Thus, it is an essential piece of the model predictive controller described in the next section. The thermal comfort model used in this paper depends on the dry-bulb air temperature. However, it is reported in the literature that in low-energy and low-exergy buildings, considering operative temperature better captures thermal comfort characteristics [19]-[20]. In [19], it is mentioned that operative temperature is a function of both dry-air bulb and mean radiant temperatures. They highlight that low exergy systems can provide desired level of thermal comfort within a safe and economic way. In [20], it is emphasized that exergetic analysis provides consistent predictions of human response to the thermal environment. Thus, it shows that energy consumption is coupled to environmental conditions, and there is a certain relation between exergy consumption and thermal comfort. In general, exergy analysis can give more information about the environment's impact on human thermal and comfort characteristics. In many studies, dry-air bulb temperature alone can be a reasonable indicator of thermal comfort since dry-air bulb and mean radiant temperature can be close to each other with low air velocity. In some other cases, however, dry-air bulb and mean radiant temperature can be significantly different when heated or cooled surfaces, thermal mass or solar radiation effects are present. Thus, in such circumstances, it can be reasonable to take account of mean radiant temperature according to thermal comfort consideration, but this would complicate the model as used in the controls algorithm. Additionally, measuring mean radiant temperature requires installing globe thermometers [21], which may be costly to implement in some low-budget retrofit solutions. Therefore, a trade-off between model accuracy and budget should be considered depending on the application.

3. CONTROLLER FORMULATION

The high-level block diagram of the overall proposed building thermostatic control architecture with weather forecast and pricing is shown in **Hata! Başvuru kaynağı bulunamadı.**3. Instead of controlling HVAC units directly, it is proposed to control the system indirectly by sending temperature set point values to the zone thermostats. This approach requires minimal hardware

changes and thus allows implementation in low-cost embedded platforms used in most of the HVAC control equipment.

In the most general form of MPC, a finite horizon optimal control problem based on a dynamic model of the process to be controlled is repeatedly solved online. In our application, the objective of the MPC controller is to find the optimal zone thermostat set points so as to reduce peak load demand in the building by exploiting the thermal dependency of building zones. To achieve this, VRF units are coordinated through virtual costs so that they do not come online at the same time. This approach is implemented by allocating lower cost time slots to each VRF unit in a rotating manner, and higher cost elsewhere. This cost will be embedded in the objective function presented in Eq. (8) below through the penalty term $Z(k)$.

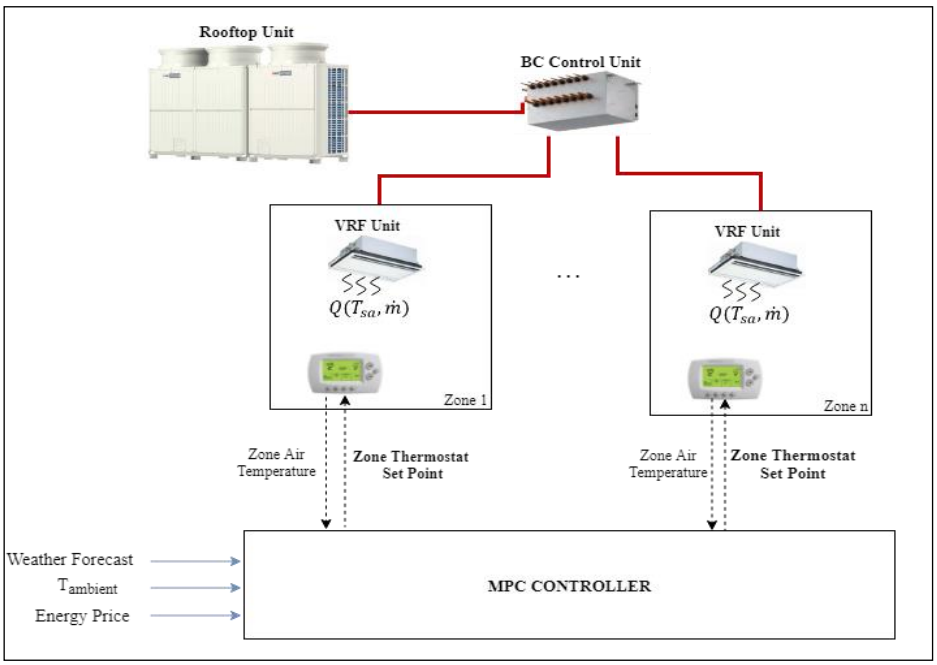

Figure 3. Building thermostatic control architecture

For controls purposes, and to make the model linear, the thermal model of the zones in Eqs. (1) and (2) is slightly modified by replacing the term $\dot{m}^j C_p^j (T_{sa}^j - T_1^j)$ in Eq. (1) with lumped heating/cooling load $Q \triangleq \dot{m}^j C_p^j (T_{sa}^j - T_1^j)$ and is treated as the main control input. Then, our new zone thermal model becomes:

$$C_1^j \dot{T}_1^j = Q + \frac{T_2^j - T_1^j}{R_1^j} + \frac{T_{oa} - T_1^j}{R_{oa}^j} + P_d^j \tag{6}$$

$$C_2^j \dot{T}_2^j = \frac{T_1^j - T_2^j}{R_1^j} + \sum_{i \in N_j} \frac{T_1^i - T_2^j}{R_{ij}} \tag{7}$$

At every control step, zone air and wall temperature measurements are taken from sensors (or from state estimation algorithms) to understand the most current status of the system dynamics. A system model similar to Eqs. (5) – (7) is then called repeatedly to predict the dynamics and constraints within a time window of several minutes. In parallel, a constrained optimization

problem in Eq. (8) is solved to obtain the optimal thermostat set points that minimize peak load and is compliant with the operating constraints within the prediction window. Then, the first set of the optimal set-point values is sent as a reference to the actuators. Finally, a new set of measurements is acquired and the whole process is repeated for the subsequent control steps.

The quadratic constrained optimization problem to compute the new thermostat set points by MPC controller is as follows:

$$\min_{Q} J = \sum_{k=1}^{N_p} \{Q(k)^T Z(k) Q(k) + \Delta Q(k)^T Z_{\Delta}(k) \Delta Q(k) + \Lambda(k)\gamma(k)\} \quad (8)$$

subject to

$$\boldsymbol{Q^{min}} \leq \boldsymbol{Q(k)} \leq \boldsymbol{Q^{max}}$$

$$\boldsymbol{T_1^{j,min}} \leq \boldsymbol{T_1^{j,k}} \leq \boldsymbol{T_1^{j,max}}$$

and Eqs. (5) – (7) are satisfied $\forall \mathbf{k}$

where

$\boldsymbol{N_p}$ is the prediction horizon, $\boldsymbol{J}$ is the zone number, $\boldsymbol{k}$ is the time step, $\boldsymbol{Q(k)} = \left[\boldsymbol{Q_k^1}, \boldsymbol{Q_k^2}, \ldots, \boldsymbol{Q_k^{n_z}}\right]$ is the set of heating/cooling loads, $\boldsymbol{\Delta Q(k)} = \left[\boldsymbol{\Delta Q_k^1}, \boldsymbol{\Delta Q_k^2}, \ldots, \boldsymbol{\Delta Q_k^{n_z}}\right]$ is the rate of change in heating/cooling loads, $\boldsymbol{T_1^{j,k}}$ is the air temperature of zone **j** at time step $\boldsymbol{k}$, $\boldsymbol{T_1^{j,min}}$ and $\boldsymbol{T_1^{j,max}}$ are the minimum and maximum air temperature constraint for zone $\boldsymbol{j}$, $\boldsymbol{Z(k)}$ is the penalty matrix on heating/cooling at time step $\boldsymbol{k}$, $\boldsymbol{Z(k)} \in \boldsymbol{R^{n_z}} \times \boldsymbol{R^{n_z}}$, $\boldsymbol{Z_{\Delta}}$ is the penalty on the rate of change in heating/cooling at time step k, is the penalty matrix on heating/cooling at time step $\boldsymbol{k}$, $\boldsymbol{\Lambda(k)}$ is the penalty on predicted percentage dissatisfied $\boldsymbol{\gamma(k)}$ at time step $\boldsymbol{k}$.

It is worthwhile to note that our MPC controller solves for optimal thermostat set-points of all zones, thus is performing a multizone optimization. This approach is capable of exploiting the thermal dynamics between different zones concurrently, and thus is more advantageous and efficient compared to standard decentralized operation where each zone is treated separately without explicit consideration of the inter-zonal dynamics. This multizone feature of our controller approaches the building HVAC optimization in a unified framework.

4. APPLICATION AND SIMULATION RESULTS

This section demonstrates the performance of the system identification and MPC formulation on MATLAB/Simulink simulations with data from a real building. In Section 4.1, the demo building and its HVAC system is described. Data collection and model identification is detailed in Section 4.2, while the performance of the MPC controller under different tuning weights are presented in Section 4.3.

4.1 Demo Building

To test our model development and controller design, a mixed-use, office and classroom building (Building T) at Yaşar University campus in İzmir was chosen. In Building T, 3 classrooms (Zones 1,3,4) and a hallway (Zone 2) from 2nd floor was considered as highlighted

in Figure 4. Building T uses a variable refrigerant flow (VRF) central heating and cooling system. The details of the thermal zones are summarized in Table 1.

Table 1. Details of zone 1-4 in building T

	Usage	Area (m^2)	Height (m)	Face	Heating Capacity (kW)	Cooling Capacity (kW)
Zone 1	Classroom	57.62	3.8	North-east	20	18
Zone 2	Hall	108.96	3.8	North-west	18	16.2
Zone 3	Classroom	60.84	3.8	South-west	25	22.4
Zone 4	Classroom	103.93	3.8	South-west	48	42

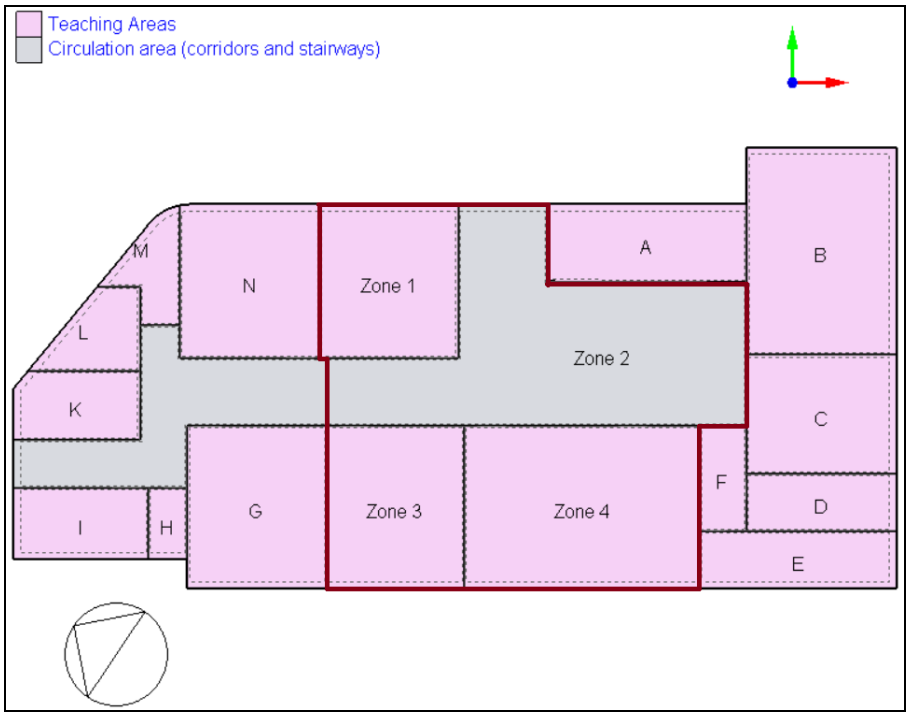

Figure 4. Building T Floor 2 layout

4.2. Thermal Model Identification

To identify the zone lumped parameter R and C values for thermal model, supply air, zone air and wall temperatures at each zone were recorded with the instrumentation setup shown in Figure 5. Measurements were collected using the TESTO Saveris-2 H1 and T3 wireless data loggers, and they are sent directly to the cloud (online data storage) via the WLAN. The data was transferred through the cloud with 1-minute intervals, which is fast enough for our slow varying thermal system. Outside dry-bulb air temperature (T_{oa}) was also measured by external sensors at the same sampling rate.

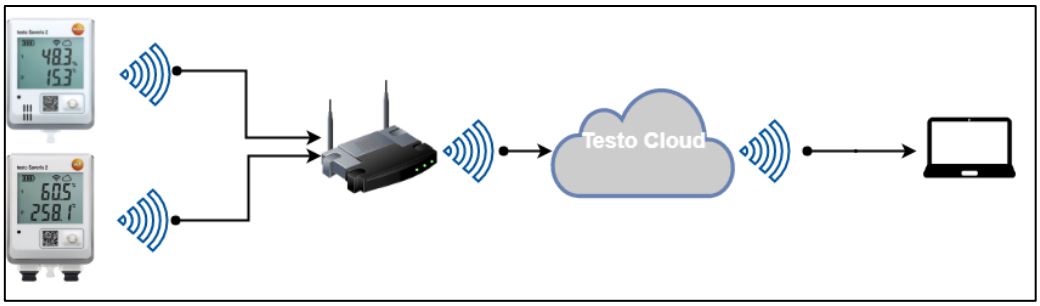

Figure 5. Instrumentation setup for zone data collection

After collecting one-day long data, the parameter identification problem in Eq. (5) was run using the input data shown in Figure 6 and the measured zone air temperature (blue) in Figure 7. The resulting R and C values are presented in Table 2, and the zone air temperatures estimated by the model are shown in Figure 7 (red).

Table 2. Parameter identification results for Zones 1-4 of Building T

Parameter	Value	Parameter	Value
C_{11}	1760.26	R_{oa1}	3.4272
C_{21}	18794.17	R_{22}	0.3294
C_{12}	7473.97	R_{23}	0.1714
C_{22}	467457.60	R_{24}	13.5480
C_{13}	3315.02	R_{oa2}	10.7485
C_{23}	84627.16	R_{33}	0.4404
C_{14}	2217.39	R_{34}	20.6000
C_{24}	7126.61	R_{oa3}	3.9676
R_{11}	0.9756	R_{44}	0.5387
R_{12}	1.0065	R_{oa4}	5.6419

As seen in Figure 7, our identified model can accurately predict the zone temperatures. Next, this model was used to design our model predictive controller, which computes optimal zone air temperature set-points.

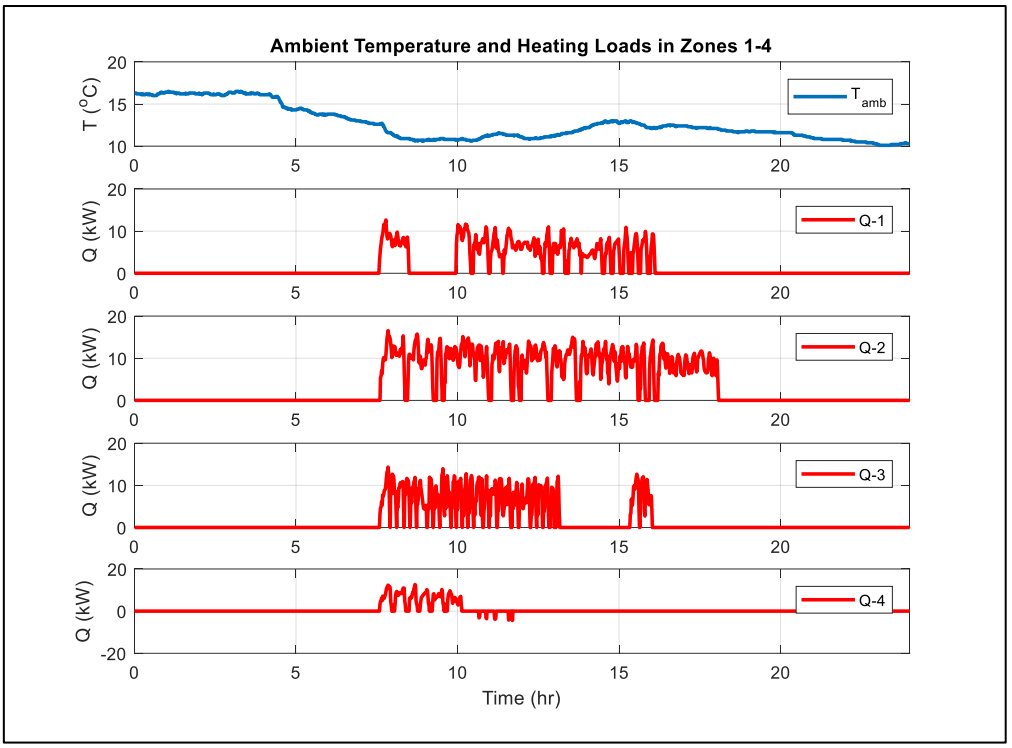

Figure 6. Ambient temperature and heating loads in zones 1-4

4.3. MPC Simulation Results

The quadratic constrained optimization problem in Eq. (8) was solved to compute optimal thermostat set-points. Two sets of simulations with different penalty weights in the objective function were performed, as summarized in Table 3.

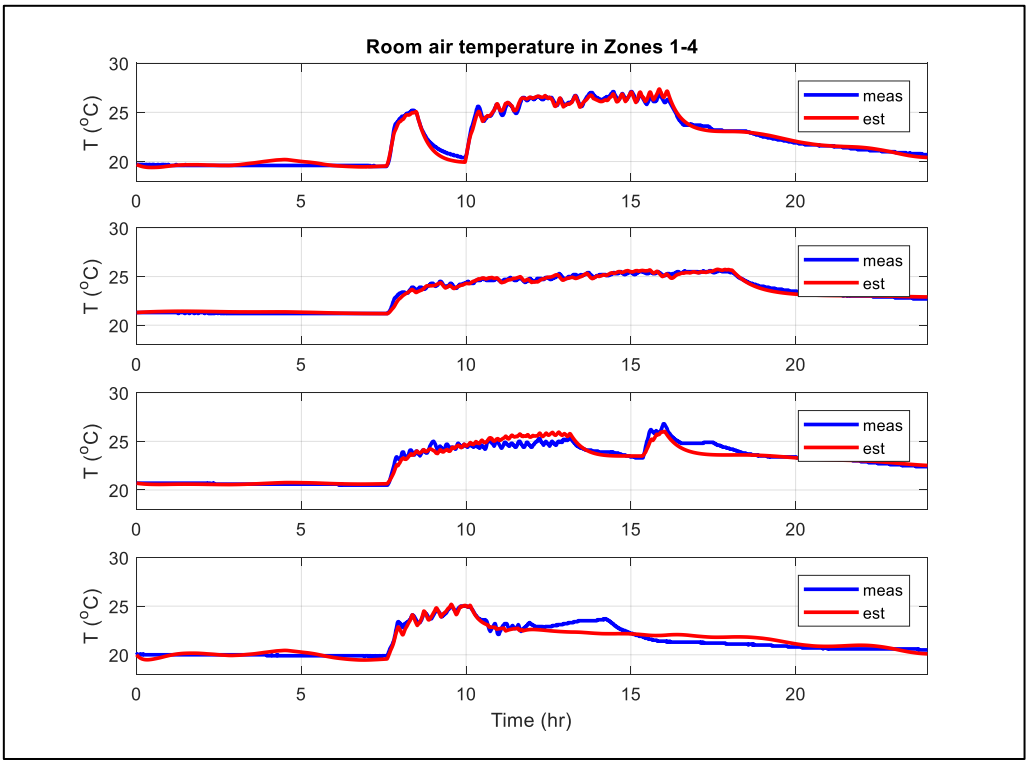

Figure 7. Room air temperature, measured and estimated

Table 3. MPC design parameters

	Case 1	**Case 2**
N_p	24 steps	24 steps
ΔT	5 minutes	5 minutes
Z	I_{4x4}	I_{4x4}
Z_Δ	0.1 x I_{4x4}	0.1 x I_{4x4}
Λ	**10 x I_{4x4}**	**100 x I_{4x4}**
Q_{max}	[20, 18, 25, 48] kW	[20, 18, 25, 48] kW
Q_{min}	[18, 16.2, 22.4, 42] kW	[18, 16.2, 22.4, 42] kW
$T_1^{j,min}$	[18, 18, 18, 18] ^oC	[18, 18, 18, 18] ^oC
$T_1^{j,max}$	[24, 24, 24, 24] ^oC	[24, 24, 24, 24] ^oC

In Case 1, thermal comfort (and implicitly zone air temperature) bounds are enforced relatively weakly compared to Case 2, as suggested by the value of the penalty term Λ in Table 3. The results of Case 1 in Figures 8-10 show a smoother heating response compared to the results of Case 2 in Figures 11-13. However, in Case 1, there exists more steady state error than Case 2 response after averaging, and higher initial overshoot in *predicted percentage dissatisfied* comfort measure. The qualitative behaviour of Case 1 may be preferable in some applications while prohibitive in some others. Therefore, proper tuning of MPC parameters is of paramount importance to achieve the desired closed loop system response. In both cases, however, the MPC controller reduces the peak load demand Q, as a quick comparison with the baseline case in Figure 6 would reveal. Thus, it can be concluded that the resulting MPC controller would bring additional peak load reduction and energy savings, thanks to its forward-looking prediction capability, which is a lacking feature in conventional HVAC controllers.

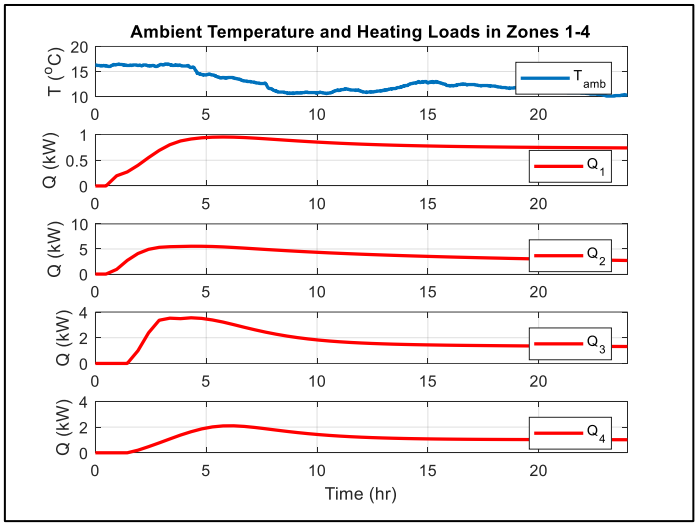

Figure 8. Ambient temperature and heating loads - Case 1

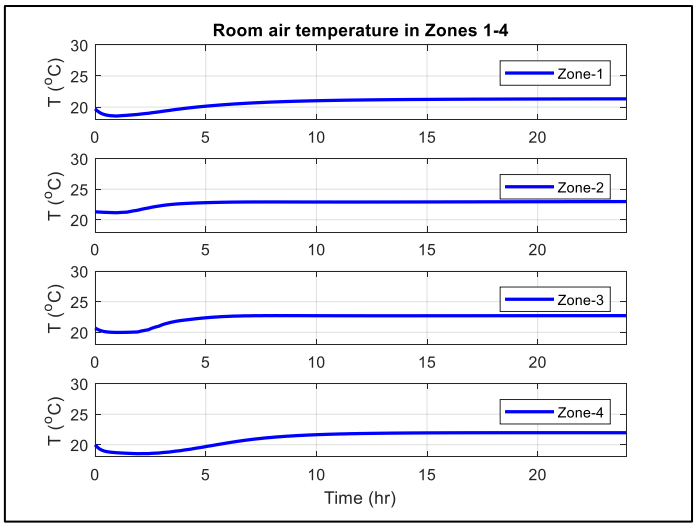

Figure 9. Room air temperature – Case 1

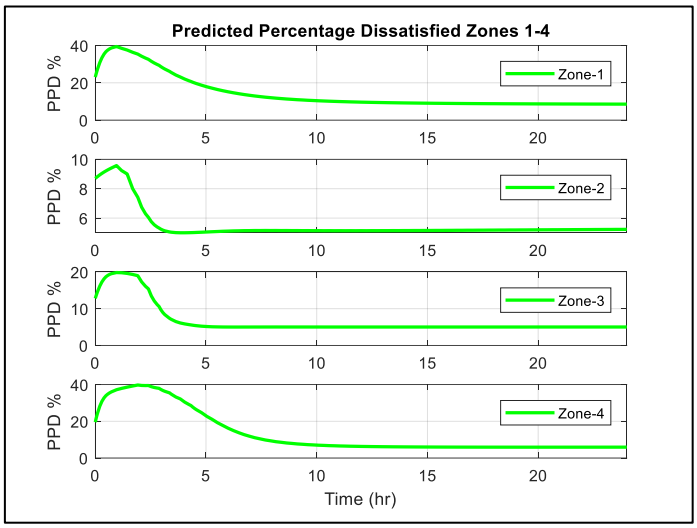

Figure 10. *Predicted percentage dissatisfied* comfort measure - Case 1

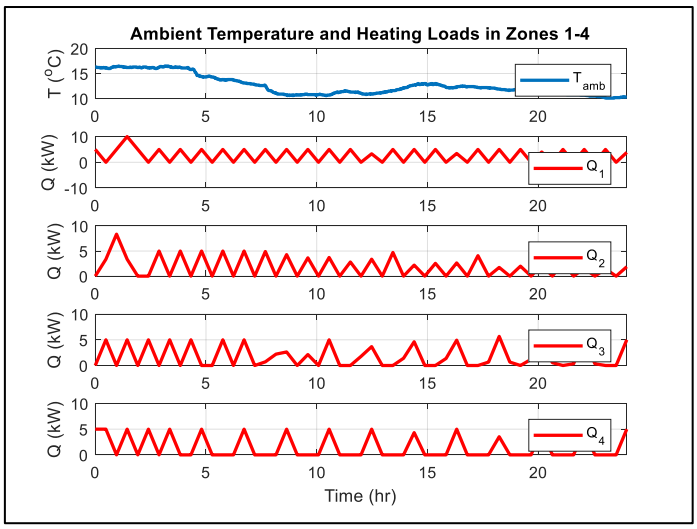

Figure 11. Ambient temperature and heating loads – Case 2

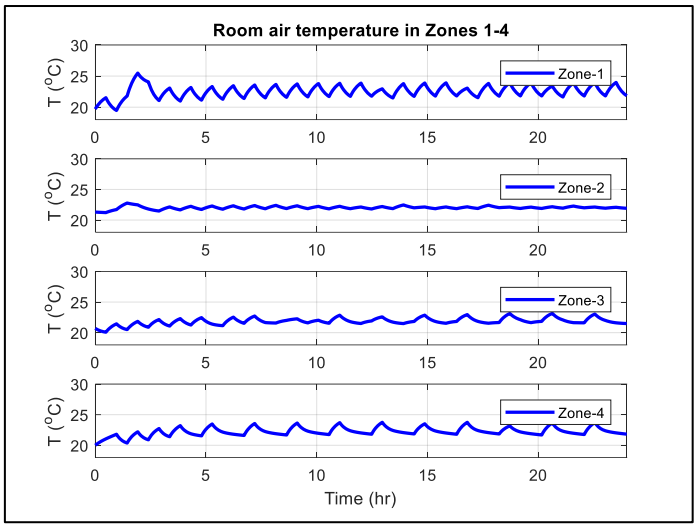

Figure 12. Room air temperature – Case 2

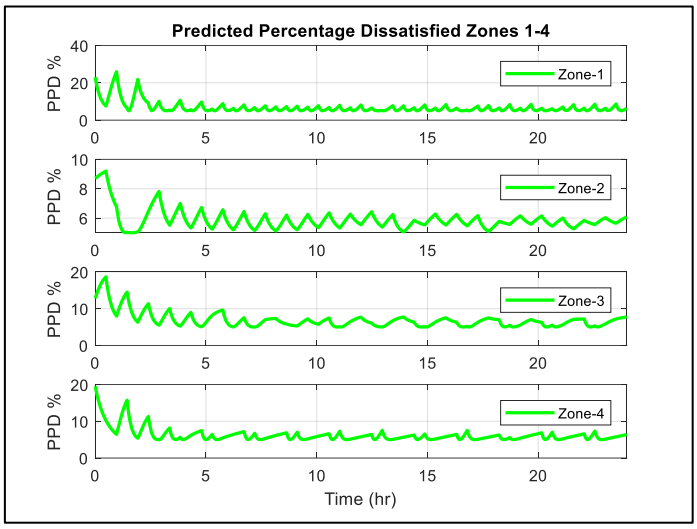

Figure 13. *Predicted percentage dissatisfied* comfort measure - Case 2

5. CONCLUSIONS

In this paper, a novel approach has been presented for reducing building peak load demand in order to enable demand response participation. The flexibility provided by the advanced controller proposed can be exploited by the building operators to offer ancillary services to the electric power grid. The technical approach includes developing a zone thermal model through system identification using real building data and model predictive control that computes optimal thermostat set-points. The developed solution can be implemented on simple or already existing equipment, therefore encouraging wider adoption of advanced building thermal control techniques. The initial simulation results show that the MPC controller achieves a smoother and a reduced heating requirement as compared to the baseline. Next steps of this research shall include tuning the MPC controller further, and implementing and testing the controller performance on the Building T at Yasar University. Another future research direction is to include, in our optimization framework, operative temperature (OT)-based thermal comfort models that are more accurate in low-energy and low-exergy buildings and addresses exergy

balance of the human body in thermal comfort with the surroundings. The additional energy savings potential of OT-based comfort will be investigated, along with energy storage capabilities of OT-based HVAC equipment like radiant panels.

NOMENCLATURE

T_1^j	air temperature of jth zone
T_2^j	wall temperature of jth zone
C_1^j	thermal capacitance of air in jth zone
C_2^j	thermal capacitance of wall in jth zone
$\dot{m}^j$	supply air mass flow rate of jth zone
C_p^j	specific heat of air in jth zone
T_{sa}^j	supply air temperature of jth zone
R_1^j	thermal resistance between air and wall in jth zone of jth zone
R_{ij}	thermal resistance between jth zone wall and adjacent ith zone air
R_{oa}^j	thermal resistance between outside air and jth zone
N_j	set of adjacents of jth zone
P_d^j	total internal disturbance heat gain
T_{oa}	outside dry-bulb air temperature
j	index of zone j
i	index of adjacent zones
n_z	number of thermal zones
P	unknown parameter vector
R	thermal resistance
C	thermal capacitance
N_s	number of samples
k	time step
$T_1^{j,m}$	measured zone air temperature of jth zone
$T_1^{j,e}$	estimated zone air temperature of jth zone from model
U	heating/cooling input vector
M	metabolic rate
L	total heat loss
W	external work
α	predicted mean vote
γ	predicted percentage dissatisfied occupants
N_p	prediction horizon
Δt	sampling period
J	zone number
Q	heating/cooling load
ΔQ	the rate of change in heating/cooling loads
Q_{max}	maximum heating load
Q_{min}	maximum cooling load
Z	penalty matrix on heating/cooling
ΔZ	penalty on the rate of change in heating/cooling
Λ	penalty on predicted percentage dissatisfied
$T_1^{j,k}$	dry-bulb air temperature of zone j

$T_1^{j,max}$ maximum dry-bulb air temperature for zone j
$T_1^{j,min}$ minimum dry-bulb air temperature for zone j

Acknowledgment

This study is supported in part by "BuildingControls – Efficient Grid Connected Buildings: A Distributed Control Framework for Managing Flexible Loads" funded by the European Commission (H2020-MSCA-IF-2015, grant agreement no: 708984).

REFERENCES

[1] Eurelectric, Power Choices- Pathways to Carbon-Neutral Electricity in Europe by 2050, Full Report, 2010.

[2] Energy Information Agency; International Energy Outlook 2011,http://www.eia.gov/forecasts/ieo/index.cfm

[3] http://www.iea.org/aboutus/faqs/energyefficiency/

[4] Directive 2010/31/EU of the Europe a Parliament And of the Council of 19 May 2010 on the Energy Performance of Buildings; 2010. Available from: http://www.epbd-ca.eu.

[5] Y. V. Makarov, L. S., J. Ma, and T. B. Nguyen, "Assessing the value of regulation resources based on their time response characteristics," Pacific Northwest National Laboratory, Richland, WA, Tech. Rep. PNNL-17632, June 2008.

[6] E. Bitar, K. Poolla, P. Varaiya. Coordinated Aggregation of Distributed Demand-Side Resources, Power Systems Engineering Research Center, Report http://pserc.wisc.edu/documents/publications/reports/2014_reports/Bitar_PSERC_Report_S-52_Dec_2014.pdf

[7] D.S. Callaway, Tapping the energy storage potential in electric loads to deliver load following and regulation, with application to wind energy, Energy Conversion and Management (50) pp. 1389–1400.

[8] H. Hao, A. Kowli, Y. Lin, P. Barooah, and S. Meyn, "Ancillary service for the grid via control of commercial building HVAC systems, American Control Conference (ACC), 2013

[9] http://www.pnnl.gov/main/publications/external/technical_reports/PNNL-22942.pdf

[10] https://www.entsoe.eu/Documents/Publications/RDC%20publications/150330_RD_Implementation_Plan_2016-2018.pdf

[11] A.I. Dounis, C. Caraiscos, Advanced control systems engineering for energy and comfort management in a building environment - A review, Renewable and Sustainable Energy Reviews, Volume 13, Issues 67, pp. 1246-1261,

[12] F. Oldewurtel, A. Parisio, C.N. Jones, M. Morari, D. Gyalistras, M. Gwerder, V. Stauch, B. Lehmann, K. Wirth, Energy efficient building climate control using stochastic model predictive control and weather predictions. In Proceedings of the 2010 American Control Conference, pp. 5100-5105, 2010.

[13] M. Yudong and G. Anderson and F. Borrelli, A distributed predictive control approach to building temperature regulation. In Proceedings of the 2011 American Control Conference, pp. 2089-2094.

[14] Zhao, J., Lam, K. P., Ydstie, B. E., & Karaguzel, O. T. (2015). EnergyPlus model-based predictive control within design–build–operate energy information modelling infrastructure. *Journal of Building Performance Simulation*, *8*(3), 121-134.

[15] Christantoni, D., Oxizidis, S., Flynn, D., & Finn, D. P. (2016). Implementation of demand response strategies in a multi-purpose commercial building using a whole-building simulation model approach. *Energy and Buildings*, *131*, 76-86.

[16] Serale, G., Fiorentini, M., Capozzoli, A., Bernardini, D., & Bemporad, A. (2018). Model Predictive Control (MPC) for Enhancing Building and HVAC System Energy Efficiency: Problem Formulation, Applications and Opportunities. *Energies*, *11*(3), 631.

[17] P.O. Fanger. Calculation of thermal comfort: Introduction of a basic comfort equation. ASHRAE Transactions, 73. Part II, pp.111.4.1-III, 4.20 (No. 2051), 1967.

[18] G. Havenith, I. Holme, and K. Parsons. Personal factors in thermal comfort assessment: Clothing properties and metabolic heat production, Energy and Buildings, 34:581-591, 2002.

[19] Djongyang, N., Tchinda, R., & Njomo, D. (2010). Thermal comfort: A review paper. *Renewable and Sustainable Energy Reviews*, *14*(9), 2626-2640.

[20] Prek, M. (2006). Thermodynamical analysis of human thermal comfort. *Energy*, *31*(5), 732-743.

[21] Kazkaz, M., & Pavelek, M. (2013). Operative temperature and globe temperature. *Engineering Mechanics*, *20*(3/4), 319-325.